

Session 0P1

Inverse Problems

Microlocal Analysis of RADAR	
<i>C. Nolan (University of Limerick, Ireland);</i>	66
Detection of Small Tumors in Microwave Medical Imaging Using Level Sets and Music	
<i>N. Irishina (Universidad Carlos III de Madrid, Spain); M. Moscoso (Universidad Carlos III de Madrid, Spain); O. Dorn (Universidad Carlos III de Madrid, Spain);</i>	67
The Mie Solution for Improving the Evolution Strategy in Breast Cancer Imaging	
<i>S. Pandaraju (University of Arkansas, USA); P. Rashidi (University of Arkansas, USA); M. El-Shenawee (University of Arkansas, USA); D. Macias (Université de Technologie de Troyes, France);</i>	72
Radiative Transport Theory for Optical Molecular Imaging	
<i>A. D. Kimn (University of California, USA);</i>	73
Reconstructing Absorption and Diffusion Shape Profiles in Optical Tomography Using a Level Set Technique	
<i>M. Schweiger (University College London, England); O. Dorn (Universidad Carlos III de Madrid, Spain); V. Kolehmainen (University of Kuopio, Finland); A. Zacharopoulos (University College London, England); S. Arridge (University College London, England);</i>	74
3D Shape Reconstruction in Optical Tomography Using Spherical Harmonics and BEM	
<i>A. Zacharopoulos (University College London, UK); S. Arridge (University College London, UK); O. Dorn (Universidad Carlos III de Madrid, Spain); V. Kolehmainen (University of Kuopio, Finland); J. Sikora (Warsaw University of Technology, Poland);</i>	75
Detection of Inclusions in the Radiative Transfer Regime	
<i>G. Bal (Columbia University, USA);</i>	80
A Parametric Level-set Approach to Tomographic Reconstruction	
<i>A. B. Tarokh (Brigham and Women's Hospital, USA); E. L. Miller (Northeastern University, USA);</i> ..	81
Shape Reconstruction in Diffuse Optical Tomography Using the Radiative Transfer Equation and Level Sets	
<i>O. Dorn (Universidad Carlos III de Madrid, Spain); M. Moscoso (Universidad Carlos III de Madrid, Spain);</i>	82
Time-reversal and Signal Subspace Methods for Imaging and Inverse Scattering of Multiply Scattering Targets	
<i>E. A. Marengo (Northeastern University, USA); F. K. Gruber (Northeastern University, USA);</i>	83
Approximation of the Scattering Coefficients for a Non-RAYLEIGH Obstacle	
<i>G. F. Crosta (Università degli Studi Milano - Bicocca, Italy);</i>	84
Three Satellite Geolocation from TDOA and FDOA Measurements	
<i>B. A. Kemp (Massachusetts Institute of Technology, USA); T. M. Grzegorzczuk (Massachusetts Institute of Technology, USA); B.-I. Wu (Massachusetts Institute of Technology, USA); J. A. Kong (Massachusetts Institute of Technology, USA);</i>	85
Inversion of Partial Information from the Polarisation Scattering Matrix in the Presence of Noise	
<i>S. Anderson (Defence Science and Technology Organisation, Australia);</i>	86

Microlocal Analysis of RADAR

C. Nolan

University of Limerick, Ireland

Microlocal analysis is a powerful mathematical tool that has developed as a refinement of geometrical optics. We will introduce it and show how to use it to analyze the scattering of radio waves (RADAR) from the earth's terrain, and how it can be used to efficiently image the earth remotely.

Detection of Small Tumors in Microwave Medical Imaging Using Level Sets and Music

N. Irishina, M. Moscoso, and O. Dorn
Universidad Carlos III de Madrid, Spain

Abstract—We focus on the application of microwaves for the early detection of breast cancer. We investigate the potential of a novel strategy using shapes for modeling the tumor in the breast. An inversion using a shape-based model offers several advantages like well-defined boundaries and the incorporation of an intrinsic regularization that reduces the dimensionality of the inverse problem whereby at the same time stabilizing the reconstruction. We explore novel level-set techniques as a means to detect the tumor without any initialization of its position and size. We present some numerical reconstructions and we compare them with the conventional MUSIC algorithm, in particular with respect to the frequency which is used for the investigation. We show that for different frequencies these two methods show a different qualitative behaviour in the reconstructions.

1. Introduction

Microwave imaging shows significant promise as a new technique for the early detection of breast cancer (see [5] and references therein). This is so because of the high contrast between the dielectric properties of the healthy breast tissue and the malignant tumors at microwave frequencies. As a consequence, microwave imaging may be used as a clinical complement to the conventional mammography which is based on the attenuation of X-rays that go through the breast. We note that mammographies offer high resolution images but with low contrast.

Several image reconstruction algorithms have been investigated during the last years for the detection and location of breast tumors using active microwave imaging. In this application, one is typically not so much interested on the detailed reconstruction of the spatial distribution of the dielectric properties (which would require by far more data than there are usually available), but mainly to answer in a fast, harmless and inexpensive way the following three questions: (i) whether or not there is a malignant tumor, (ii) its (approximate) location, and (iii) its (approximate) size. Once these questions have been answered reliably, more details can be investigated if necessary by alternative (but then typically more expensive) imaging techniques.

In this paper we investigate the use of the level set technique (see [4, 7–11] and references given there for details) as a means to detect the presence, location and size of small tumors if their properties are assumed to be known. The main difficulty in this work is the extremely limited view to the domain of interest due to a very specific source-receiver geometry: all sources and receivers are located at the same side of the domain. Our observation from earlier work [4] has been that in these situations the level set iteration, when initiated with an arbitrary starting guess for the shape, tends to suffer from local minima, which makes it difficult to reliably detect the correct location of the tumor. Therefore, we have investigated an adaptation of our level set approach to this new situation which is able to start without any pre-specified starting guess for the shape. Our algorithm is able to create shapes in any location of the domain. It does so during the early iterations taking into account the data and the sensitivity mapping of the inverse problem. Once a good first approximation for the shape is found, it continues in a completely automatic way with optimizing this shape until the data least squares cost functional is sufficiently reduced. We compare the results of numerical experiments for this new reconstruction algorithm with those of a straightforward (and non-optimized) implementation of the MUSIC algorithm (for a detailed theoretical and numerical investigation of this imaging scheme see for example [1–3, 6] and the references given there). Some conclusions of this comparison are given at the end of this paper.

2. Level Set Formulation of the Problem

For modelling TM-waves in Microwave imaging we use a scalar Helmholtz equation for $u(\mathbf{x})$ describing one component of the electric field. It is

$$\Delta u + \kappa(\mathbf{x})u = q(\mathbf{x}) \quad \text{in } \Omega = \mathbb{R}^2 \quad (1)$$

with $\kappa(\mathbf{x}) = \omega^2 \mu_0 \epsilon_0 \left[\epsilon(\mathbf{x}) + i \frac{\sigma(\mathbf{x})}{\omega \epsilon_0} \right]$. The field u is required to satisfy the Sommerfeld radiation condition, and it is assumed to be continuous together with its normal derivatives across interfaces. In the shape inverse problem

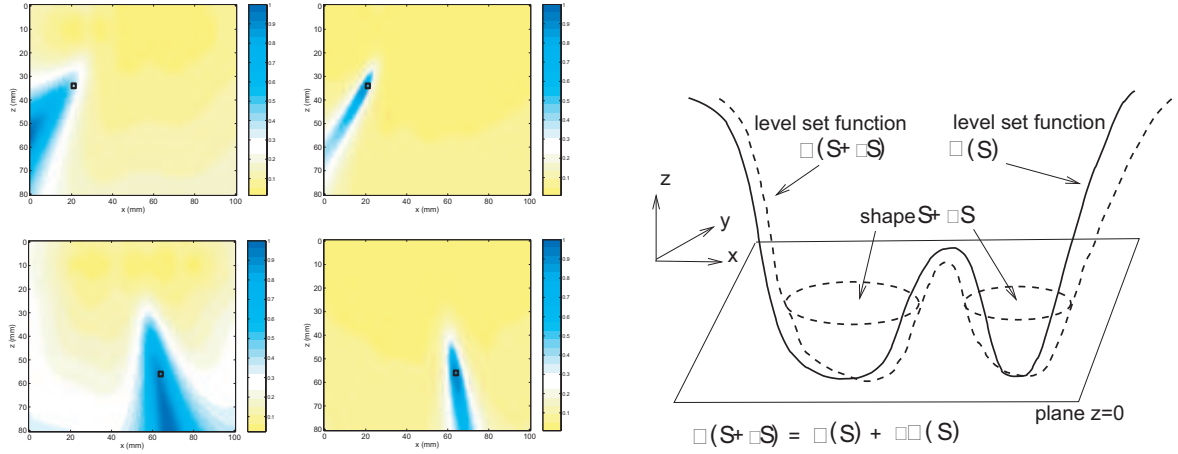


Figure 1: Left: The MUSIC estimate (10), normalized to one, of the location of one tumor in a homogeneous medium. The exact location and the size of the $2 \times 2 \text{ mm}^2$ tumor is denoted by the square. The tumor is located less deeper in the top row than in the bottom one. The frequencies used in these images are 3 GHz (left column) and 4 GHz (right column). Right: Evolution of a shape by a level set formulation.

we assume that the parameter distribution is described by

$$\kappa(\mathbf{x}) = \begin{cases} \kappa_i & \text{in } S \\ \kappa_e & \text{in } \Omega \setminus S \end{cases} \quad (2)$$

where S defines the shape of the tumor. For the formal derivation of our reconstruction approach we introduce the one-dimensional Heaviside function $H(\psi)$ which is defined as $H(\psi) = \begin{cases} 1 & , \psi > 0 \\ 0 & , \psi \leq 0 \end{cases}$. We call ψ a *level set representation of the shape S* if

$$\kappa(\psi) = \kappa_e H(\psi) + \kappa_i (1 - H(\psi)). \quad (3)$$

Using the level set representation, $\psi(\mathbf{x})$ the shape S is characterized by all those points $\mathbf{x} \in \Omega$ where $\psi(\mathbf{x}) \leq 0$, and the region $\Omega \setminus S$ is characterized by those points $\mathbf{x} \in \Omega$ where $\psi(\mathbf{x}) > 0$ (see Fig. 1 on the right). The boundary of the shape S is then modeled by the zero level set $\partial S = \{\mathbf{x} \in \Omega : \psi(\mathbf{x}) = 0\}$. It is clear that the level set representation of a given shape S is not unique. However, every continuous function ψ uniquely specifies a corresponding shape (which we denote $S[\psi]$) by the above definitions. We now define the least squares data misfit cost functional $\mathcal{J}(\psi) = \frac{1}{2} \|\mathcal{R}(\kappa(\psi))\|^2$, where $\mathcal{R}(\kappa(\psi))$ denotes the difference between measured data and those calculated by a forward solver using the parameter distribution κ (modeled by the level set function ψ). The goal during the shape reconstruction problem will be to find an evolution of the level set functions ψ in artificial evolution time t which reduces and eventually minimizes this cost functional. We consider the general evolution law

$$\frac{d\psi}{dt} = f(\mathbf{x}, t, \psi, \mathcal{R}, \dots) \quad (4)$$

for the level set function ψ describing the shape S during the artificial evolution. Then the unknown which we are looking for is the forcing term $f(\mathbf{x}, t, \psi, \mathcal{R}, \dots)$, which might depend on a variety of parameters as indicated. Formally differentiating (3) with respect to ψ yields $\frac{d\kappa}{d\psi} = (\kappa_e - \kappa_i)\delta(\psi)$ where $\delta(\psi) = H'(\psi)$ is the one-dimensional Dirac delta distribution. Formally differentiating the least squares cost functional $\mathcal{J}(\kappa(\psi(t)))$ with respect to the artificial time variable t and applying the chain rule yields

$$\frac{d\mathcal{J}}{dt} = \text{Re} \int_{\Omega} \mathcal{R}'_i(\kappa)^* \mathcal{R}(\kappa) (\kappa_e - \kappa_i) \delta(\psi) f(\mathbf{x}, t, \psi, \mathcal{R}, \dots) d\mathbf{x}, \quad (5)$$

where Re indicates the real part of the corresponding quantity. In (5), $\mathcal{R}'_i(\kappa)^*$ denotes the formal adjoint of the linearized Residual operator $\mathcal{R}'_i(\kappa)$ and the expression $\mathcal{R}'_i(\kappa)^* \mathcal{R}(\kappa)$ coincides with the pixel-based Fréchet

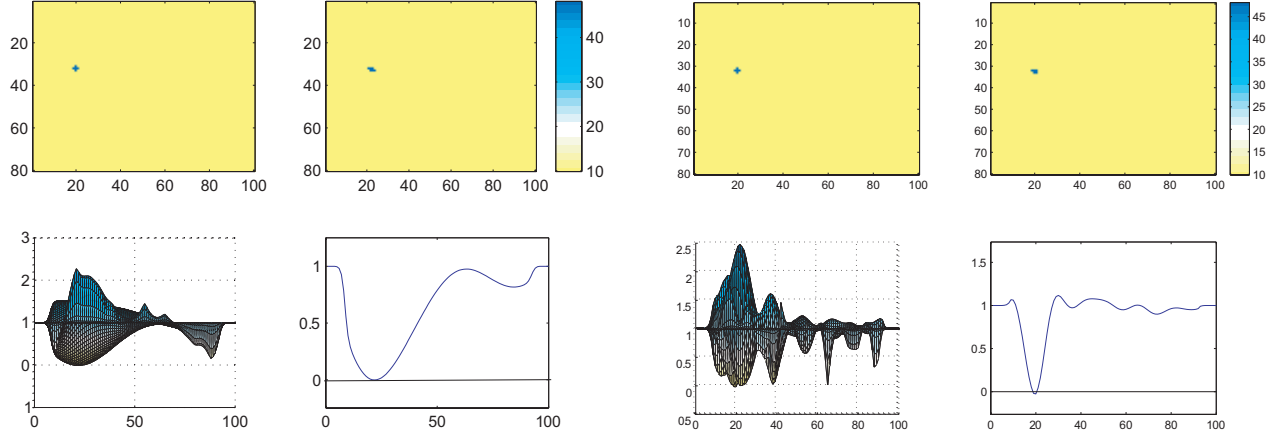


Figure 2: Reconstruction of a small tumour with the level set formulation. Left: using frequency 1 GHz. Right: using frequency 4 GHz. More details can be found in the text.

derivative of the parameter-to-data mapping of the corresponding parameter reconstruction problem [10]. Using the fact that formally $\delta(\psi) > 0$ in (5), we can define the search or descent direction as

$$f_d(\mathbf{x}) = -\text{Re}((\kappa_e - \kappa_i) \mathcal{R}'_l(\kappa) * \mathcal{R}(\kappa)) \quad \text{for all } \mathbf{x} \in \Omega. \quad (6)$$

In contrast to more traditional level set approaches which typically use a Hamilton-Jacobi-type formulation, our search direction $f_d(\mathbf{x})$ has the property that it can be applied even if there is no initial shape available when starting the algorithm. Therefore, it allows for the creation of objects at any point in the domain, by lowering a positive level set function until its values arrive at zero. This property is useful for avoiding certain types of local minima which often occur in level set formulations which are solely based on the propagation of an already existing shape. Numerically discretizing (4) by a straightforward finite difference time-discretization with time-step $\tau > 0$ and interpreting $\psi^{(n+1)} = \psi(t + \tau)$ and $\psi^{(n)} = \psi(t)$ yields the iteration rule

$$\psi^{(n+1)} = \psi^{(n)} + \tau f_d(\mathbf{x}), \quad \psi^{(0)} = \psi_0. \quad (7)$$

3. MUSIC formulation of the problem

We consider an array of N electromagnetic transducers located at positions \mathbf{x}_n , $n = 1, 2, \dots, N$. Two adjacent transducers are separated by a distance $\lambda_0/2$, where λ_0 denotes the wavelength of the signal emitted by the array. With this arrangement the transducers do not behave like separate entities but like an array having an aperture $a = (N - 1)\lambda_0/2$ that interrogates the medium. Within the medium there are M targets (tumors) located at positions \mathbf{y}_m , $m = 1, \dots, M$. The scattered echos by the tumors are recorded at the array. We call the resulting data set the multistatic response matrix (MSR matrix) $K = (K_{ij})$, whose entries are defined by the scattered field detected at the i th transducer (in receive mode) when the j th transducer (in active mode) emits an electromagnetic signal. The goal is to estimate the location \mathbf{y}_m of the tumors from the knowledge of the MSR matrix. The singular value decomposition of the MSR is given by

$$K = U \Sigma V^H, \quad (8)$$

where the superscript H denotes the hermitian matrix. In (8), Σ is a diagonal matrix whose diagonal entries σ^2 are the eigenvalues of the time reversal matrix (TR matrix) $T = K^H K$. If there are less targets than array elements ($M < N$) there are at most M non zero eigenvalues indexed from 1 to M , and $N - M$ zero eigenvalues indexed from $M + 1$ to N . The column vectors of the matrix U in (8), denoted by \mathbf{U}_k ($k = 1, \dots, N$), are the eigenvectors of $T = K^H K$ normalized to one. The column vectors of V , denoted by \mathbf{V}_k ($k = 1, \dots, N$), are the complex conjugates of \mathbf{U}_k . It can be shown that the N dimensional space of signal vectors applied to the N element antenna array can be expressed as the direct sum $\mathcal{S} \oplus \mathcal{N}$ [6]. The signal subspace \mathcal{S} can be spanned by the significant eigenvectors of the TR matrix T , i.e., by \mathbf{U}_k with $k = 1, \dots, M$, while the null space

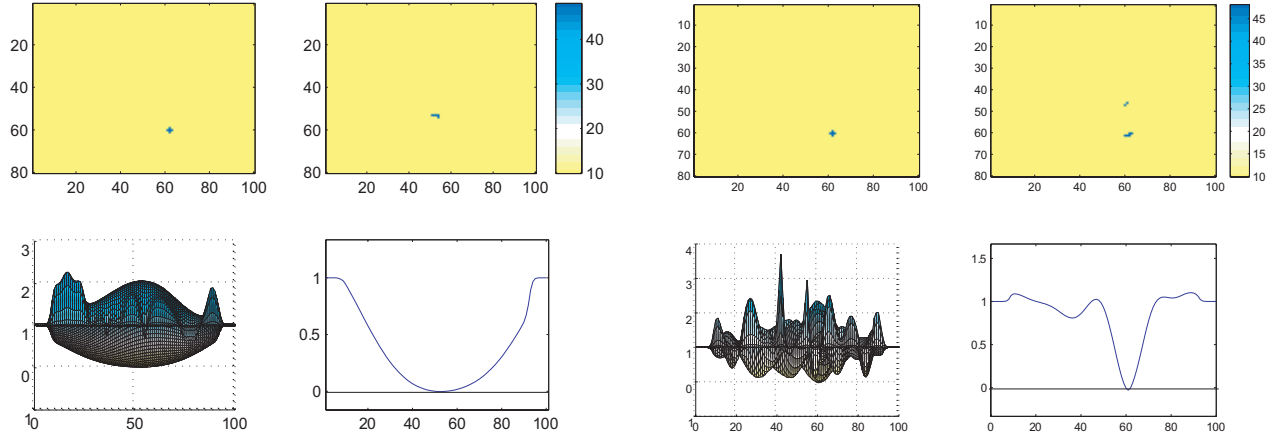


Figure 3: Reconstruction of a small tumour with the level set formulation. Left: using frequency 1 GHz. Right: using frequency 4 GHz. More details can be found in the text.

\mathcal{N} is spanned by those eigenvectors having zero eigenvalues, i. e., by \mathbf{U}_k with $k = M + 1, \dots, N$. The MUSIC algorithm exploits the fact that the MSR matrix is a projection operator onto the signal subspace \mathcal{S} which is also spanned by the complex conjugates of the vectors

$$g(\mathbf{y}_m) = (G(\mathbf{x}_1, \mathbf{y}_m), G(\mathbf{x}_2, \mathbf{y}_m), \dots, G(\mathbf{x}_N, \mathbf{y}_m))^t, \quad (9)$$

where $m = 1, \dots, M$, the superscript t denotes the transpose, and $G(\mathbf{r}, \mathbf{r}')$ is the deterministic two-point Greens function of the background medium. Therefore, we have that $\langle \mathbf{U}_k, g^*(\mathbf{y}_m) \rangle$ for $k = M + 1, \dots, N$. Then, we can display the objective functional

$$\mathcal{F}(\mathbf{y}^s) = \frac{1}{\sum_{k=M+1}^N |\langle \mathbf{U}_k, g^*(\mathbf{y}^s) \rangle|^2} \quad (10)$$

for the search points \mathbf{y}^s in the domain. Since $g^*(\mathbf{y}^s)$ is orthogonal to \mathbf{U}_k , with $k = M + 1, \dots, N$, whenever the search point \mathbf{y}^s equals a tumor location, (10) will exhibit a peak at those positions. We will normalize (10) to one. We note that

$$\sum_{k=M+1}^N |\langle \mathbf{U}_k, g^*(\mathbf{y}^s) \rangle|^2 = |g^*(\mathbf{y}^s) - \sum_{k=1}^M (\mathbf{U}_k^t g^*(\mathbf{y}^s)) \mathbf{U}_k^*|^2. \quad (11)$$

Since in our application we will consider only one tumor ($M = 1$) it is more efficient to compute $\mathcal{F}(\mathbf{y}^s) = (|g^*(\mathbf{y}^s) - (\mathbf{U}_1^t g^*(\mathbf{y}^s)) \mathbf{U}_1^*|^2)^{-1}$, normalized to one, instead of (10).

4. Numerical Experiments

In the numerical experiments shown here, the domain of investigation consists of (simulated) tissue of the size $10 \times 8 \text{ cm}^2$ in which a tumour of size $2 \times 2 \text{ mm}^2$ is imbedded at different positions as shown in Figs. 2 and 3. The relative electric permittivity values are 9 in the background medium and 49 inside the tumor. For simplicity, the conductivity value is assumed here to be a small constant of value 0.001 S/m everywhere in the medium. 8 transducers are equidistantly positioned at the top side of the medium. They illuminate the medium with microwaves of different frequencies (we use here 1, 3 and 4 GHz). We solve (1) with a second order finite differences scheme and a perfectly matching layer (PML). The received numerical data have been perturbed by 5 % white Gaussian noise. Fig. 1 shows on the left the MUSIC estimate for the two target locations. In the top row the target is located at a less deep position than in the bottom row. We have used frequencies of 3 GHz (left column) and 4 GHz (right column). Figs. 2 and 3 show the estimates of the level set based algorithm for the two different locations of the hidden tumor. Each of these two figures is divided into two panels of 4 subfigures (the left panel shows results for frequency 1 GHz and the right one for 4 GHz). Each panel of figures is structured in the following way. Top left: true permittivity distribution; top right: reconstructed permittivity

distribution; bottom left: final level set function viewed from the side; bottom right: horizontal cross section of the final level set function through the location of the recovered tumor.

5. Observations and Conclusions

We observe in our numerical experiments that the MUSIC algorithm provides a good estimate of the cross-range for high frequencies (4 GHz) with a resolution that decreases with depth (compare the top right and bottom right images of Fig. 1). However, range information is lost (in particular at the deep location), and therefore it should be obtained separately. See for example Ref. [2]. For a lower frequency (3 GHz) both, range and cross-range resolution decrease. For frequencies lower than 3 GHz we were not able to get useful estimates of the tumor locations with the MUSIC algorithm.

On the other hand, the level set based reconstruction scheme shows a somehow reversed behavior compared to the MUSIC results. For lower frequencies (here 1 GHz) it shows a quite stable estimate of the approximated tumor location, whereas for higher frequencies (here 4 GHz) the corresponding oscillations in the electromagnetic fields tend to introduce artifacts in the reconstructions. As a consequence, the estimate using the level set algorithm gives rise to a ghost location of the tumor in addition to its correct location. We note that the resolution provided for the level set algorithm is much better than that given by the MUSIC algorithm. We also want to mention here that the level set reconstruction method has also the potential of iteratively finding the contrast values of the tumors from the given data if they are not a-priori known. Although this has not been implemented so far in our algorithm, some related approaches can be seen in [7, 10–11]. The MUSIC algorithm is not easily extendable to incorporate this feature.

We conclude that level set based algorithms can provide a useful and flexible strategy for the early detection of small tumors in tissue with microwaves. In the future we plan to extend our method to the more complex situation in which the dielectric properties of the healthy tissue and the tumor are unknown and need to be reconstructed from the given data.

Acknowledgment

This work has been supported by the Ministerio de Educación y Ciencia of Spain, grant FIS2004-03767.

REFERENCES

1. Ammari, H. and I. Eakovleva, "Lesselier d 2005 a music algorithm for locating small inclusions buried in a half-space from the scattering amplitude at a fixed frequency," *SIAM Multiscale Mod. Sim.*, Vol. 3, No. 3, 597–628.
2. Berryman, J., L. Borcea, G. Papanicolaou, and C. Tsogka, "Statistically stable ultrasonic imaging in random media," *J. Acoust. Soc. Am.*, Vol. 112, 1509–1522, 2002.
3. Borcea, L., G. Papanicolaou, C. Tsogka, and J. Berryman, "Imaging and time reversal in random media," *Inverse Probl.*, Vol. 18, 1247–1279, 2002.
4. Dorn, O., E. Miller, and C. rappaport, "A shape reconstruction method for electromagnetic tomography using adjoint fields and level sets," *Inverse Problems*, Vol. 16, 1119–1156, 2000.
5. Fear, C. E., S. C. Hagness, P. M. Meaney, M. Okoniewski, and M. A. Stuchly, "Breast tumor detection," *IEEE Microwave Mag.*, 48–56, March 2002.
6. Gruber, F. K., E. A. Marengo, and A. J. Devaney, "Time-reversal imaging with multiple signal classification considering multiple scattering between the targets," *J. Acoust. Soc. Am.*, Vol. 115, No. 6, 3042–3047, 2004.
7. Litman, A., "2005 reconstruction by level sets of n -ary scattering obstacles," *Inverse Problems*, Vol. 21, 1–22.
8. Ramananjaona, C., M. Lambert, and D. Lesselier, "Shape inversion from TM and TE real data by controlled evolution of level sets," *Inverse Problems*, Vol. 17, 1585–1595, 2001.
9. Santosa, F., "A level set approach for inverse problems involving obstacles," *ESAIM Control, Optimization and Calculus of Variations*, Vol. 1, 17–33, 1996.
10. Schweiger, M, S. R. Arridge, O. Dorn, A. Zacharopoulos, and V. Kolehmainen, "2005 Reconstructing absorption and diffusion shape profiles in optical tomography using a level set technique," accepted by *Optics Letters*.
11. Tai, X. C. and T. F. Chan, "A survey on multiple level set methods with applications for identifying piecewise constant functions," *International Journal of Numerical Analysis and Modeling*, Vol. 1, No. 1, 25–47, 2004.

The Mie Solution for Improving the Evolution Strategy in Breast Cancer Imaging

S. Pandalraju, P. Rashidi, and M. El-Shenawee
University of Arkansas, USA

D. Macias
Université de Technologie de Troyes, France

In a previous work in microwave imaging, we have successfully characterized three-dimensional malignant breast cancer tumors employing evolution strategies. Particularly, we determined the form (with a number of unknowns dependent on the irregularity of the shape) and the location (three unknowns) of non-spherical tumors from scattering data. However, notwithstanding the encouraging results obtained, the iterative nature of the imaging method required several CPU hours on a Hewlett-Packard AlphaServer DS25. In this work we propose a strategy to speed up the imaging process through an improvement of the initialization of the evolutionary search.

An evolution strategy is a heuristic population-based optimization technique, inspired on the Darwinian principles of variation and selection, which searches the best fit solution through the exploration of a search space with the assistance of a forward solver and a fitness functional. The variation stage includes the recombination and mutation operations and is responsible for the increase in the variety of the search space. The selection process retains those elements of the population leading to more promising regions of the search space. The evolutionary loop continues until a convergence criterion has been fulfilled.

Instead of generating the initial population employing uniformly distributed random numbers, we initialize the evolution strategy with a population estimated by means of Mie's scattering theory. This approach is valid in the sense that tumors can be considered, at least in principle, as lossy spheres immersed in a homogeneous lossy medium. Thus, a decrease in the computing time required by the evolution strategy and method of moments imaging method could be expected since the search space has been reduced to a region in the neighborhood of the optimum.

Our preliminary results obtained employing the approach described above show potential in achieving convergence at a faster rate. Some issues related to the error sensitivity are also discussed in this work.

Radiative Transport Theory for Optical Molecular Imaging

A. D. Kimn

University of California, USA

We study the inverse fluorescent source problem for optical molecular imaging in tissues. We use the radiative transport equation to model light propagation in tissues. In particular, we make use of analytical results for a point source and a voxel source to compute estimates for the location and size of a general fluorescent source in a halfspace composed of a uniform absorbing and scattering medium. We present numerical results demonstrating this theory.

Reconstructing Absorption and Diffusion Shape Profiles in Optical Tomography Using a Level Set Technique

M. Schweiger¹, O. Dorn², V. Kolehmainen³, A. Zacharopoulos¹, and S. Arridge¹

¹University College London, England

²Universidad Carlos III de Madrid, Spain

³University of Kuopio, Finland

A novel shape reconstruction algorithm for optical tomography is presented which is based on a level-set formulation for the shapes. The goal is to recover contrast and shapes of inclusions in the absorption as well as in the scattering/diffusion parameter simultaneously from boundary data. Evolution laws based on descent directions for a cost functional are derived for two different level-set functions, one describing the absorption and one the diffusion parameter, as well as for the parameter values inside these shapes. Numerical experiments are presented in 2-D which show that the new method is able to simultaneously recover shapes and contrast values of absorbing and scattering objects embedded in a slightly heterogeneous background medium from simulated noisy data. These results are compared with more traditional pixel-based reconstructions, of which the regularization parameter is determined by an L-curve method. It is shown that, using this regularization parameter, the pixelbased reconstructions are severely smeared-out over a relatively large domain, such that contrast values and sizes of the objects are not well recovered. Compared to these pixel-based reconstructions, the shape-based inversions deliver a very good guess for the shapes, and the contrast values are recovered with higher accuracy.

3D Shape Reconstruction in Optical Tomography Using Spherical Harmonics and BEM

A. Zacharopoulos¹, S. Arridge¹, O. Dorn², V. Kolehmainen³, and J. Sikora⁴

¹University College London, UK

²Universidad Carlos III, Spain

³University of Kuopio, Finland

⁴Warsaw University of Technology, Poland

Abstract—We consider the recovery of smooth 3D region boundaries with piecewise constant coefficients in Optical Tomography (OT). The method is based on a parametrisation of the closed boundaries of the regions by spherical harmonic coefficients, and a Newton type optimisation process. A boundary integral formulation is used for the forward modelling. An advantage of the proposed method is the implicit regularisation effect arising from the reduced dimensionality of the inverse problem. Results of a numerical experiment are shown which demonstrate the performance of the new method in a realistic situation.

1. Introduction

In this paper, we explore a technique for the retrieval of the internal boundaries of 3D regions in frequency domain Diffusive Optical Tomography (DOT), [3]. The optical parameter of interest in this application are μ_a being the absorption coefficient, μ'_s being the (reduced) scattering coefficient, and their combination $D = \frac{1}{3(\mu_a + \mu'_s)}$ being the diffusion coefficient. They are assumed to take piecewise constant values in the three dimensional bounded domain Ω with jumps at the interior interfaces. There are several physiologically interesting observations which can be derived from the knowledge of the absorption and diffusion of light in tissue. This includes tissue oxygenation, blood volume and blood oxygenation [1, 2]. Primary applications are the detection and classification of tumourous tissue in the breast, monitoring of the oxygenation level in infant brain tissue, and functional brain activation studies.

Our model for light propagation in biological tissue is the diffusion equation [3]

$$-\nabla \cdot D(\mathbf{r})\nabla\Phi(\mathbf{r}) + \mu_a(\mathbf{r})\Phi(\mathbf{r}) + \frac{i\omega}{c}\Phi(\mathbf{r}) = \mathbf{q}(\mathbf{r}) \quad (1)$$

where $\Phi(\mathbf{r})$ is photon density, c is the speed of light in the medium, and $q(\mathbf{r})$ describes the source term. It represents the number of photons per unit volume at the source position \mathbf{r} . ω is the modulation frequency. The appropriate boundary condition is of the Robin type (given by (4)). However, if we assume that the distribution of the optical parameters inside the body Ω is arranged into L disjoint regions Ω_j , so that $\Omega = \bigcup_{j=1}^L \Omega_j$, which are separated by smooth closed interfaces Γ_j , and have piecewise constant optical properties $\{D_j, \mu_{a,j}\}$, we may describe the propagation of light by a set of coupled Helmholtz equations

$$-\Delta\Phi_j + k_j^2\Phi_j = q_j \quad \text{in } \Omega_j, \quad (2)$$

with boundary conditions

$$\Phi_{j+1} = \Phi_j, \quad D_{j+1} \frac{\partial\Phi_{j+1}}{\partial\nu} = D_j \frac{\partial\Phi_j}{\partial\nu} \quad \text{on } \Gamma_j, \quad (3)$$

$$\Phi_1 + 2AD_1 \frac{\partial\Phi_1}{\partial\nu} = 0 \quad \text{on } \partial\Omega. \quad (4)$$

Here, A models the refractive index difference at the boundary $\partial\Omega$. The respective (complex) ‘wavenumbers’ are $k_j^2(\omega) = \frac{\mu_{a,j} + \frac{i\omega}{c}}{D_j}$.

The described inverse problem of 3D DOT is severely ill-posed due to the diffusive behavior of the fields in the tissue and the relatively small number of available noisy data. This typically leads to quite unstable reconstructions, unless strong regularization is applied. One possible way of regularizing the problem is to take advantage of prior information about the general structure of the expected parameter distribution, which often is available in medical applications from alternative imaging modalities or from general anatomical knowledge.

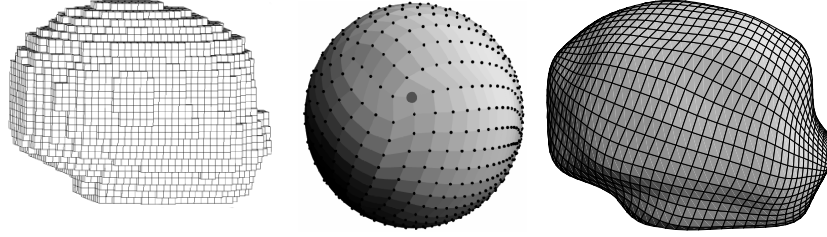


Figure 1: Segmented MRI data of a baby's scalp and as voxel volume (left), (Thanks to Richard Bayford, Middlesex University). The mapping of the surface on the sphere (middle). The parametric representation with 11 degrees of spherical harmonics (right).

This will be our approach in this paper, assuming that the domain of interest can be divided into basically two different zones: a background distribution and an embedded object whose shape can be approximately described by a given (small) number of spherical harmonics parameters.

2. Parametric Representation of Surfaces

Our main interest lies in the use of geometric prior information in order to create a sufficiently realistic model of the different subregions of an anatomical structure. Having in mind applications in head and brain imaging, we decided to use the head's geometry as a test bed. We can use good resolution MRI or CT-scan images as prototypes. Both imaging modalities use voxel maps to create an image. The voxel faces comprising the boundary surface are mapped to the surface of a sphere by a method described in [9].

Since our application is not limited to star-shaped objects, a harmonic distribution of the extracted surface's net onto the sphere's surface was chosen instead of a direct radial function. Having defined coefficients $\{C_l^m\}$, we can use them to create the parametric description of the surface by weighted averaging with the relevant spherical harmonics

$$v = \begin{cases} v_x(\vartheta, \varphi) &= \sum_{l=0}^{\varpi} \sum_{m=-l}^l C_{l,x}^m Y_l^m(\vartheta, \varphi), \\ v_y(\vartheta, \varphi) &= \sum_{l=0}^{\varpi} \sum_{m=-l}^l C_{l,y}^m Y_l^m(\vartheta, \varphi), \\ v_z(\vartheta, \varphi) &= \sum_{l=0}^{\varpi} \sum_{m=-l}^l C_{l,z}^m Y_l^m(\vartheta, \varphi). \end{cases} \quad (5)$$

Here, ϖ is the maximum degree of spherical harmonics that we used for the particular representation. In practice, to ensure that only real surfaces are represented, we define a real basis as

$$\tilde{Y}_l^m(\vartheta, \varphi) := \begin{cases} \operatorname{Re}[Y_l^m](\vartheta, \varphi), & \text{when } m \leq 0, \\ \operatorname{Im}[Y_l^m](\vartheta, \varphi), & \text{when } m > 0, \end{cases} \quad (6)$$

for which the orthogonal condition $\langle \tilde{Y}_l^m, \tilde{Y}_{l'}^{m'} \rangle = \delta_{mm'} \delta_{ll'}$ still holds. For simplicity we introduce the notation $\gamma_j = \{C_l^m\}_j$, with $l = 1, \dots, \varpi$ and $m = -l, \dots, l$ which describes the finite set of spherical harmonics coefficients for the surface Γ_j up to degree ϖ .

3. The Forward Problem

As in conventional pixel based reconstruction we assume multiple sources p_s , $s = 1, \dots, S$ and detectors m_d , $d = 1, \dots, M$, located at the surface $\partial\Omega$. During the experiment, light is emitted from one source at a time and the photons leaving the domain are collected at all the detectors. We denote by $g_{s,d}$ the measurements which corresponds to detector d and source s . The combined measurements for a source s are denoted by \mathbf{g}_s . A boundary integral formulation is used to simplify the discretisation of the volume of the domain Ω to that of the interfaces Γ_j of the disjoint regions that comprise Ω . The shapes and locations of the boundaries are described by finite sets of shape coefficients $\gamma = \{\gamma_j\}$. The forward problem uses a Boundary Element Method (BEM) to discretise the mapping from the shape coefficients $\{\gamma_j\}$ and the optical parameters values $\{D_j, \mu_{a,j}\}$ to the data $\mathbf{g} = \mathcal{M}(\gamma)\Phi$ on the surface $\partial\Omega$, where \mathcal{M} denotes the linear measurement operator which typically takes point evaluations of the fields Φ at few discrete points of the surface $\partial\Omega$. The inverse problem in this setup amounts to finding the representation $\{\gamma_j\}$ and the values $\{D_j, \mu_{a,j}\}$ from observed or simulated measurements \mathbf{g} .

Discretising our forward problem (2)–(4) by the so-called ‘collocation Boundary Element Method’ [4, 8] we construct a linear matrix equation of the form

$$\mathbf{T}(\gamma)\mathbf{f} = \mathbf{q} \quad (7)$$

The matrix $\mathbf{T}(\gamma)$ (which depends in a nonlinear way on the shape parameters γ) takes the form of a dense non-symmetric block matrix. The corresponding system is solved using a preconditioned GMRES solver. To relate the BEM approach to the forward model, we introduce the linear measurement operator \mathcal{M} . Then we have

$$\mathbf{g}_s = \mathcal{K}_s(\gamma, D, \mu_a) = \mathcal{M}\mathbf{T}^{-1}(\gamma)\mathbf{q}_s, \quad (8)$$

where \mathbf{g}_s are the measured data at the discrete points m_d , $d = 1, \dots, M$ corresponding to the source \mathbf{q}_s , and $\mathcal{K}_s(\gamma, D, \mu_a)$ denotes the nonlinear forward operator mapping unknown shape parameters to the corresponding measurements [3]. In the following we will omit the subindex s in the notation for simplicity.

4. The Shape Inverse Problem

Starting from a geometric configuration defined by the set of shape coefficients (γ^0), we will try to search for the set (γ^*) that minimises the distance between computed data $\mathcal{K}(\gamma, D, \mu_a)$ and given data \mathbf{g} . Our approach will be a cost minimisation procedure:

$$\text{find } \gamma^* \text{ so that } \Xi(\gamma^*) = \min_{\gamma} \|\mathbf{g} - \mathcal{K}(\gamma, D, \mu_a)\|^2 \quad (9)$$

A typical way to minimise such a cost function is a Newton-type method, [7], where we search for a minimum for $\Xi(\gamma)$ by iterations of local linearisation and Taylor expansion around the current estimate γ^k as

$$\gamma^{k+1} = \gamma^k + (\mathbf{J}_k^T \mathbf{J}_k + \Lambda)^{-1} \mathbf{J}_k^T (\mathbf{g} - \mathcal{K}(\gamma^k, D, \mu_a)). \quad (10)$$

Λ is a Levenberg-Marquandt control term [5]. In our implementation, we take Λ to be the identity.

The modified Newton method (10) for the minimisation of the residual (9) produces the descent direction in the parameter space by providing a step $\delta\gamma^k = \gamma^{k+1} - \gamma^k$. In practice, moving $\Xi(\gamma)$ to the full step length $\delta\gamma^k$ could lead the residual far from the actual minimum. A quadratic fit line search method is introduced in order to avoid detours in the downhill direction and speed up the optimisation.

5. Construction of the Jacobian

One of the key elements in the implementation of the optimisation scheme (10) is the calculation of the Jacobian $\mathbf{J} = \frac{\partial \mathcal{K}(\gamma, D, \mu_a)}{\partial \gamma}$ of the forward operator \mathcal{K} with respect to the shape coefficients γ . Since the measurement operator \mathcal{M} is linear, this amounts essentially with (8) to calculating $\frac{\partial \mathbf{T}(\gamma)^{-1}}{\partial \gamma_i}$ in an efficient way. In our numerical calculations we have implemented a semi-adjoint scheme for calculating these expressions. Assume that the matrix \mathbf{T} is invertible and differentiable with derivative $\frac{\partial \mathbf{T}(\gamma)}{\partial \gamma_i}$. Differentiation of the identity $\mathbf{T}(\gamma)^{-1} \mathbf{T}(\gamma) = \mathbf{I}$ yields by the product rule

$$\frac{\partial \mathbf{T}(\gamma)^{-1}}{\partial \gamma_i} = -\mathbf{T}(\gamma)^{-1} \frac{\partial \mathbf{T}(\gamma)}{\partial \gamma_i} \mathbf{T}(\gamma)^{-1} \quad (11)$$

Denote $\mathbf{f}_s = \mathbf{T}(\gamma)^{-1} \mathbf{q}_s(\gamma)$ the solution vector for the s^{th} source vector by $\mathbf{q}_s(\gamma)$, and let $\mathbf{e}_d = [0 \ 0 \ \dots \ 0 \ 1 \ 0 \ \dots \ 0 \ 0]$ the standard d^{th} unit vector where the value 1 is at d^{th} position. Then, the measurement at the d^{th} detector corresponding to source s can be written as

$$g_{sd} = \mathbf{e}_d^T \cdot \mathbf{f}_s = \mathbf{e}_d^T \cdot \mathbf{T}(\gamma)^{-1} \cdot \mathbf{q}_s(\gamma) \quad (12)$$

By differentiation with respect to γ_i and using the identity (11) we get

$$\frac{\partial g_{sd}}{\partial \gamma_i} = \mathbf{e}_d^T \cdot \mathbf{T}^{-1}(\gamma) \cdot \frac{\partial \mathbf{T}(\gamma)}{\partial \gamma_i} \cdot \mathbf{T}^{-1}(\gamma) \cdot \mathbf{q}_s(\gamma) + \mathbf{e}_d^T \cdot \mathbf{T}^{-1}(\gamma) \cdot \frac{\partial \mathbf{q}_s(\gamma)}{\partial \gamma_i} \quad (13)$$

Denoting furthermore

$$\mathbf{f}_d^+ = \mathbf{e}_d^T \cdot \mathbf{T}^{-1}(\gamma), \quad \mathbf{Q}_s = \mathbf{T}^{-1}(\gamma) \cdot \frac{\partial \mathbf{q}_s(\gamma)}{\partial \gamma_i} \quad (14)$$

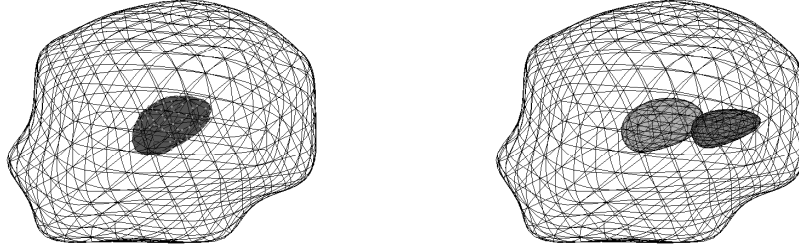


Figure 2: Recovery of inhomogeneity shape from OT measurements on the surface with known a-priori optical parameters. (left) the target; (right) red: the initial guess, green: the reconstructed shape.

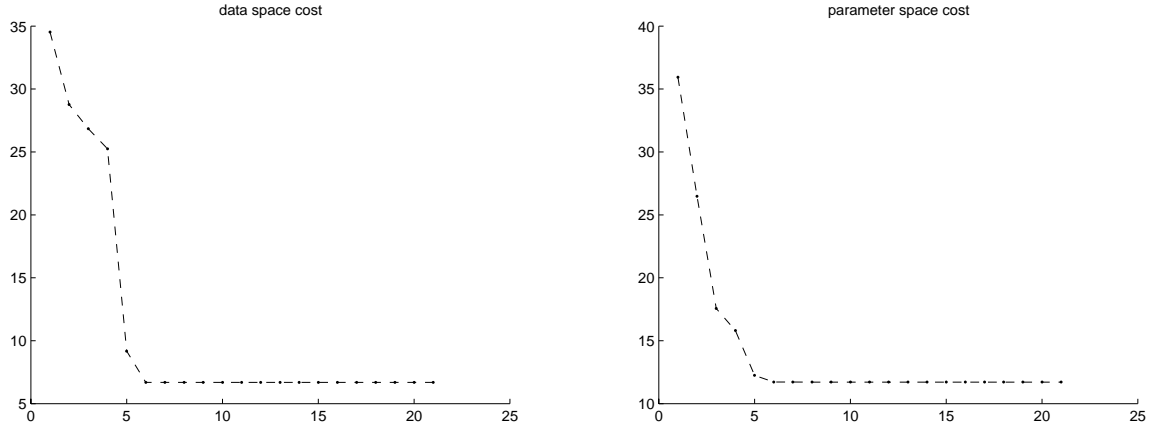


Figure 3: Relative data error, $\|\mathbf{g}^{-1}(\mathbf{g} - \mathcal{K}(\gamma_k, D, \mu_a))\|$ on the left, and parameter space error $\sum_n \|(\gamma_{target,n} - \gamma_{k,n})\|^2$, on the right.

we finally arrive at

$$\frac{\partial g_{sd}}{\partial \gamma_i} = \mathbf{f}_d^{+,T} \cdot \frac{\partial \mathbf{T}(\gamma)}{\partial \gamma_i} \cdot \mathbf{f}_s + \mathbf{e}_d^T \cdot \mathbf{Q}_s. \quad (15)$$

We notice that $\frac{\partial g_{sd}}{\partial \gamma_i}$ are the actual entries of the Jacobian \mathbf{J} . The derivative of the BEM system matrix \mathbf{T} with respect to the geometrical parameter γ_i is now done using a finite difference method

$$\frac{\partial \mathbf{T}(\gamma)}{\partial \gamma_i} = \frac{\mathbf{T}(\gamma_1, \dots, \gamma_i + \varepsilon_i, \dots, \gamma_n) - \mathbf{T}(\gamma_1, \dots, \gamma_i, \dots, \gamma_n)}{\varepsilon_i} \quad (16)$$

The practical choice of ε_i requires a trade-off between the mathematical accuracy of the derivative approximation and the computer roundoff error consideration [7]. In our case it is chosen empirically as $10^{-4}\gamma_i$.

6. Results from 3D Simulations

In our experimental setup, a geometric model for an infant's head (Figure 1) is created and treated as a homogeneous domain with an embedded randomly shaped inhomogeneity, which we try to recover. The optical parameters chosen for the homogeneous background are $\mu_a = 0.01 \text{ cm}^{-1}$ and $\mu_s = 1 \text{ cm}^{-1}$, and for the internal region Ω_2 we have $\mu_a = 0.05 \text{ cm}^{-1}$ and $\mu_s = 2. \text{ cm}^{-1}$. The inhomogeneity's surface is described by 16 spherical harmonic coefficients γ_0 for each cartesian coordinate x , y , z . This defines a parametric surface using up to the 3^{rd} degree spherical harmonics. A regular mesh with 48 elements and 98 nodes is mapped onto that surface to create the discrete approximation necessary for the BEM calculation, see Figure 2.

Using this geometric setup, we assign 20 sources and 20 detector positions at the surface of the head. The modulation frequency on the sources is set to 100 MHz. Synthetic data are then collected at the 20 detectors using the forward model $\mathcal{K}(\gamma_0)$ with one source illuminated at a time. We split this data into real and imaginary parts of its logarithm to get a vector $\mathbf{g} \in \mathbb{R}^{800}$. Gaussian random noise with a standard deviation of 1% of the

measured signal is added to these data. As the initial guess for the reconstruction we select a closed surface centred at a random position. In this case, we use 9 parameters for each direction in a 2nd degree spherical harmonics description. This choice leads to a search space of dimension $3 \times 9 = 27$. The solution follows the residual minimisation technique described above. The reconstructed boundary is displayed in Figure 2. Figure 3 shows the relative data error $\|\mathbf{g}^{-1}(\mathbf{g} - \mathcal{K}(\gamma_k, D, \mu_a))\|$ versus iteration index k on the left hand side. On the right hand side of this figure, a measure for the quality of the approximation of the shape is displayed. Due to the larger number of coefficients γ_0 used for the construction of the target than for the definition of the evolution shape γ_k , we define γ_{target} to be the set of spherical harmonics coefficients that define the target truncated up to the degree used for the evolution. So the residual of Figure 3 is chosen to be $\sum_n \|(\gamma_{target,n} - \gamma_{k,n})\|^2$, with n summing up to the degree of spherical harmonics used for the evolution shape.

As can be seen, the location and the approximate shape of the simple 3D homogeneous region can be recovered with good accuracy from noisy data. The minimisation of the least squares functional has completed successfully with the distance norm becoming 33 times smaller than the initial value after only 5 iterations. On the other hand, the distance between the shape coefficients shows good convergence if we take into account that a different degree of spherical harmonics was used for the creation of the simulated data than for the evolving shape during the reconstruction.

7. Conclusion

In the paper we have proposed a novel reconstruction scheme for a shape based three dimensional inverse problem in DOT. In our method, the search space for the solution of the inverse problem is defined in terms of a spherical harmonic expansion of the unknown region surfaces which are not restricted being star-shaped. Doing so we incorporate in our scheme an implicit regularisation, where the regularisation parameter is the degree of spherical harmonics used for representing the surfaces. A semi-adjoint formulation of the parameter- or shape-sensitivities has been derived. In our numerical experiments, using the semi-adjoint form, we have demonstrated that our scheme is able to reconstruct in a stable and efficient way low-parametric approximations of more complicated shapes from few given data.

Acknowledgment

Support from the European Union in the 6th framework program under the contract LSHG-CT-2003-503259 and EPSRC GR/R86201/01 is gratefully acknowledged.

REFERENCES

1. Yodh, A. G. and D. A. Boas, *Biomedical photonics handbook*, CRC Press, 2003.
2. Gibson, A. P., J. C. Hebden, and S. R. Arridge, "Recent Advances in Diffuse optical imaging," *Phys. Med. Biol.*, Vol. 50, 1–43, 2005.
3. Arridge, S. R., "Optical tomography in medical imaging," *Inverse Problems*, Vol. 15, 41–93, 1999.
4. Becker, A. A., *The Boundary Element Method in Engineering-a Complete Course*, McGraw-Hill Book Company, 1992.
5. Marquardt, D. W., "An algorithm for least-squares estimation of nonlinear parameters," *J. Soc. Industrial Math.*, Vol. 11, No. 2, 431–441, 1963.
6. Bonnet, M., "Bie and material differentiation applied to the formulation of obstacle inverse problems," *Eng. Anal. with Boundary Elements*, Vol. 15, 121–136, 1995.
7. Vogel, C. R., "Computational methods for inverse problems," *Frontiers in Applied Mathematics Series*, Vol. 23, SIAM, 2002.
8. Sikora, J., A. Zacharopoulos, A. Douiri, M. Schweiger, L. Horesh, S. Arridge, and J. Ropoll, "Diffuse photon propagation in multilayered Geometries," *Phys. Med. Biol.*, 2005.
9. Brechbühler, C., G. Gerig, and O. Kübler, "Parameterization of closed surfaces for 3-D shape description," *Com. Vis. and Image Understanding*, Vol. 61, No. 2, 154–170, 1995.

Detection of Inclusions in the Radiative Transfer Regime

G. Bal

Columbia University, USA

Inclusions can be modeled as variations in the constitutive parameters of radiative transfer equations for the energy density of waves propagating in highly heterogeneous media. In the practically useful regime where the inclusions have a small volume compared to the overall size of the system, we present asymptotic expansions that characterize the influence of the inclusions on available measurements and show how these formulas may be used towards detection and imaging. These asymptotic formulas are also compared with numerical simulations of the wave equation, where the inclusions are modeled as either void areas (where fluctuations are suppressed) or perfectly reflecting objects. Careful numerical simulations of wave equations in two space dimensions over domains of size comparable to 500 wavelengths allow us to assess the volume of the inclusions that can be detected and imaged from the available measurements. This is joint work with Olivier Pinaud.

A Parametric Level-set Approach to Tomographic Reconstruction

A. B. Tarokh

Brigham and Women's Hospital, USA

E. L. Miller

Northeastern University, USA

We consider an approach to the tomographic reconstruction problem based on a parametric form of the level-set method to describe the geometry of a 3D object. Inspired by the flexibility and simplicity of linear expansion methods that are commonplace in the signal processing and applied mathematics literatures, our method makes use of such expansions in the description of the level-set function. Given a fixed set of basis functions, the level-set function is described using a linear combination of these basis functions, with the expansion coefficients treated as unknowns. Our formulation admits the use of a wide range of basis functions, and we provide several specific examples of bases to demonstrate the method's flexibility (polynomial, sinusoidal, and Gaussian). A non-linear optimization method is developed for determining the optimal values of the unknowns. In addition to the level-set function expansion coefficients, we also estimate the space-varying textures of the anomaly and background. Modelling these features using linear expansions (similarly to the level-set function), we include the corresponding expansion coefficients in the non-linear optimization routine. Hence, our algorithm simultaneously optimizes the structure of the anomaly as well as the space-varying textures of the anomaly and background. Finally, to enforce an overall smoothness of the reconstructed target, we include in our optimization process a regularization term that penalizes the surface area of the target.

Our geometric approach to the tomographic imaging problem is an efficient, parametric technique that sequentially "evolves" the two-dimensional surface that bounds the modelled anomalous region of interest. The tomographic flow, or surface evolution, is affected through iterative cost-decreasing steps using a gradient-based evolution of the parameters that define the surface as well as the textures. The cost functional is defined as a typical log likelihood functional arising from the assumed Gaussian nature of the noise corrupting the observed data. The key attractive features of our approach are as follows: 1) Our model admits the presence of multiple spatially-separate anomalous regions in the medium. 2) We employ an appropriate regularization penalty to improve the robustness of the algorithm in the presence of noise. This penalty has the effect of encouraging a smooth reconstructed shape. 3) The simple characterization of the object in terms of a low number of parameters lends itself to efficient computational implementation.

The flexibility afforded by the use of basis expansion functions requires a method for determining those that should in fact be used in the reconstruction given a large dictionary of options. This would imply that we simultaneously optimize over a vector of coefficients equal in cardinality to the dictionary of basis function, which is computationally intractable even for modestly-sized dictionaries. Hence, we seek to retain the advantages of having a large dictionary of basis functions for representing the level-set function corresponding to our anomalous region, while maintaining an overall tractable optimization. To this end, we introduce a greedy algorithm for selecting a small set of basis functions that yield improved cost, where the cost functional is retained from the non-adaptive case above.

We validate our approach through extensive numerical studies on simulated noisy data generated using X-ray and diffuse optical tomographic (DOT) models.

Shape Reconstruction in Diffuse Optical Tomography Using the Radiative Transfer Equation and Level Sets

O. Dorn and M. Moscoso

Universidad Carlos III de Madrid, Spain

We consider Diffuse Optical Tomography as an inverse problem for the radiative transfer equation in 2D. The goal is to find and characterize small objects embedded in a heterogeneous medium. We assume that we know certain characteristics of the background medium, as for example average values of the absorption and scattering coefficient, but small fluctuations of a reasonable amount are assumed to be unknown. The optical parameters inside the embedded objects (e.g., tumors or other anomalies) are assumed to be significantly different from the background values and constant, but their values (as well as the shapes of the objects) are unknown. The region of interest is surrounded by a band of clear fluid (e.g., CFL), which is assumed to be non-scattering or very low-scattering. The data consist then of the time-dependent outgoing photon flux at discrete receivers located at the boundary of the domain. A level set strategy is employed in order to find the topology, the shapes as well as the contrast of the unknown inclusions. Several numerical examples are presented which demonstrate the performance of the method in various situations.

Time-reversal and Signal Subspace Methods for Imaging and Inverse Scattering of Multiply Scattering Targets

E. A. Marengo and F. K. Gruber
Northeastern University, USA

In this work the inverse scattering problem of estimating the locations and scattering strengths of a number of multiply scattering point targets in the near or far field from single-snapshot active antenna array data is investigated with the aid of two signal subspace approaches: Time-reversal-based methods with an emphasis on time-reversal multiple signal classification (MUSIC) and a new signal subspace method developed in this work that is based on parameter search in high-dimensional parameter space. The second approach corresponds under additive white Gaussian noise to the maximum likelihood (ML) estimator for the target positions in the (distorted wave) Born approximated case. The approach also corresponds to the ML estimator for the multiple scattering case so long as the associated forward and inverse problems are treated in terms of an equivalent two-point scattering potential matrix or tensor instead of the one-point scattering potential function or the target reflectivities.

The methods are comparatively investigated, and it is found that for weakly interacting targets whose collective scattering is describable by the Born approximation the ML method outperforms the time-reversal approach in number of localizable targets, being it possible, e.g., to locate up to $N(N+1)/2-1$ or N^2-1 targets using coincident or non-coincident arrays of N transmitters and receivers, respectively, instead of the time-reversal limit of only up to $N-1$ targets. The number of targets that are in principle localizable using the time-reversal MUSIC approach remains unchanged under Born-approximable versus non-Born-approximable (exact, multiple scattering) conditions. On the other hand, if multiple scattering is significant then the high-dimensional search method yields a less dramatic advantage over the time-reversal approach in number of localizable targets. The high-dimensional signal subspace method is also found to yield better resolution performance at the expense of higher computational demand.

A new explicit formula (a non-iterative algorithm) to calculate the scattering strengths once the target locations have been determined is also developed which holds even in the nonlinear regime of multiply scattering targets. The approach is valid so long as the conditions for applicability of the time-reversal approach for generally non-coincident arrays are met, in particular, $M \leq \min(N_t, N_r)$ and $M < \max(N_t, N_r)$ where N_t and N_r are the number of transmitters and receivers, respectively, and M is the number of point targets.

The final part of the presentation includes extensions of the previous algorithms for the case of extended targets where instead of a single Green function vector or propagator per target there is an effectively finite-dimensional subspace of such propagators. The paper includes computer-simulated validations of the theory which comparatively address the performance of the methods.

The work reported in this presentation expands previous work co-authored by the present authors on time-reversal imaging and inverse scattering of multiply scattering point targets, with the main contributions of the present work residing in the development of a non-iterative formula for the full nonlinear inverse scattering reconstruction and in the comparative investigation of time-reversal in the context of alternative signal subspace approaches (the ML approach included) for the associated target localization problem with active arrays. This work also goes a step beyond in considering the generalization of these developments to extended targets.

REFERENCES

1. Gruber, et al., *J. Acoust. Soc. Am.*, Vol. 115, No. 6, 3042–3047, June 2004.
2. Devaney, et al., *J. Acoust. Soc. Am.*, Vol. 118, No. 5, November 2005.

Approximation of the Scattering Coefficients for a Non-RAYLEIGH Obstacle

G. F. Crosta

Università degli Studi Milano - Bicocca, Italy

Let $\Omega \subset \mathbb{R}^2$ be a star shaped obstacle with smooth boundary, Γ . Let u denote the incident scalar plane wave and v the scattered wave complying with $(u + v)|_{\Gamma} = 0$ and the SOMMERFELD radiation condition. Let λ denote a pair of indices and $\{u_{\lambda}\}$ be the family of real wave functions, which is linearly independent and complete in $L^2(\Gamma)$, provided $k^2 \notin \sigma[-\Delta_D]$ (the wavenumber squared is not an eigenvalue of the interior DIRICHLET LAPLACE operator). The scattering coefficients are defined by $f_{\lambda} = -(i/4)\langle u_{\lambda} | \partial_N(u + v) \rangle$, where $\partial_N(\cdot)$ is the outward normal derivative on Γ and $\langle \cdot | \cdot \rangle$ denotes the inner product in $L^2(\Gamma)$.

If L denotes the approximation order and $\Lambda[L]$ the related set of indices, approximate scattering coefficients $\{p_{\lambda}^{(L)}\}$ can be introduced

$$p_{\lambda}^{(L)} = -(i/4)\langle u_{\lambda} | \partial_N u + (\partial_N v)_2^{(L)} \rangle \quad (1)$$

with

$$(\partial_N v)_2^{(L)} = \sum_{\mu \in \Lambda[L]} c_{\mu}^{(L)} \partial_N v_{\mu}. \quad (2)$$

Here $F_2 = \{\partial_N v_{\mu}\}$ is the family of normal derivatives of outgoing waves $\{v_{\mu}\}$, which is unconditionally complete, and $\{c_{\mu}^{(L)}\}$, $\mu \in \Lambda[L]$, are suitable expansion coefficients. Let $W \equiv \{w_{\mu}\}$ denote a family of functions such that

$$w_{\mu} = (1/2)\partial_{N[\mathbf{r}]}v_{\mu} + (i/4) \int_{\Gamma} \partial_{N[\mathbf{r}]}H_0^{(1)}[kR] \partial_{N[\rho]}v_{\mu} d\Gamma[\rho], \quad (3)$$

where $R = |\mathbf{r} - \rho|$.

The following results can be shown to hold.

- 1) The family W is linearly independent and complete in $L^2(\Gamma)$ provided $k^2 \notin (\sigma[-\Delta_D] \cup \sigma[-\Delta_N])$ i.e., k^2 is neither an eigenvalue of the interior DIRICHLET nor of the interior NEUMANN LAPLACE operators.
- 2) The coefficients $\{c_{\mu}^{(L)}\}$, which form the vector $\mathbf{c}^{(L)}$ of card $[\Lambda[L]]$ components, solve the well-posed algebraic system

$$\mathbf{W}^{(L)} \cdot \mathbf{c}^{(L)} = \mathbf{g}^{(L)}, \quad (4)$$

where $\mathbf{W}^{(L)} = [\langle w_{\lambda} | w_{\mu} \rangle]$ is the GRAMian of $\{w_{\mu}\}$ and $\mathbf{g}^{(L)} = [\langle g | w_{\mu} \rangle]$ is a vector of known terms obtained from

$$g = (1/2)\partial_{N[\mathbf{r}]}u - (i/4) \int_{\Gamma} \partial_{N[\rho]}u \partial_{N[\mathbf{r}]}H_0^{(1)}[kR] d\Gamma[\rho]. \quad (5)$$

- 3) Finally, an error estimate for $\|\partial_N v - (\partial_N v)_2^{(L)}\|_{L^2(\Gamma)}^2$ can be provided in terms of the smallest eigenvalue of a double layer acoustic potential.

RAYLEIGH's hypothesis is nowhere required i.e., both F_2 and W only have to be linearly independent and complete.

Three Satellite Geolocation from TDOA and FDOA Measurements

B. A. Kemp, T. M. Grzegorzczuk, B.-I. Wu, and J. A. Kong
Massachusetts Institute of Technology, USA

Geolocation refers to the localization of an emitter from measurements by passive receivers (satellites) at known locations. We consider the problem of three satellites used for determining the location of an electromagnetic source that is known to be on or near the surface of the Earth. Typically, the multilateration solution is obtained from time-difference-of-arrival (TDOA) measurements. In this configuration, one of the three satellites is designated as the reference such that two TDOA equations are obtained by subtracting the time-of-arrival (TOA) measurements of the reference satellite from the TOA measurement of the non-reference satellites. Therefore, the three satellite case is underdetermined for the three dimensional (3D) localization problem (i.e., there are two equations and three unknowns $u = [x, y, z]^T$). The introduction of an altitude constraint, for example restricting the source location to the surface of the Earth, yields one additional equation such that the problem is critically determined. However, the true altitude of the source may not be known exactly due to variations of the Earth's surface from sea level. When there is relative motion between the source and receivers, the Doppler shift gives two frequency-difference-of-arrival (FDOA) equations. Thus, there are four (two TDOA and two FDOA) equations that can be used to determine the three source location coordinates. The three satellite geolocation problem is then overdetermined. We present a solution to the three satellite geolocation problem based on iterative linearization of the TDOA and FDOA equations. We show that the resulting iterative maximum likelihood estimator (ML) achieves the Cramer-Rao Lower Bound (CRLB) in low measurement noise, but the likelihood of nonconvergence increases with measurement noise. Furthermore, we demonstrate that introduction of a source altitude constraint decreases the estimator variance below the unconstrained CRLB and increases the numerical robustness for higher measurement noise. However, it is shown that error in the altitude constraint projects bias onto the estimated source location vector.

Inversion of Partial Information from the Polarisation Scattering Matrix in the Presence of Noise

S. Anderson

Defence Science and Technology Organisation, Australia

Consider the following scattering scenario. An unidentified scatterer Q_i from a known class Q is moving on a trajectory $\Gamma_{Q_i}(t)$ in R^3 and illuminated in the Fraunhofer zone by a class of sources T moving on trajectories $\Gamma_{T_k}(t)$. The sources radiate distinct rest-frame signals $\Phi_{T_k}(t) \cdot \hat{\pi}_{T_k}(\theta, \phi)$ which are scattered by Q_i according to the scattering matrix $\tilde{S}_{Q_i}(\vec{k}_{sc}, \vec{k}_{inc})$ in Q_i 's rest-frame. Here $\hat{\pi}_{T_k}(\theta, \phi)$ represents the polarisation state of the signal radiated by T_k in its local rest-frame direction (θ, ϕ) .

A class of (noisy) receivers R moving on trajectories $\Gamma_{R_j}(t)$ sample the scattered signals

$$\vec{Z}^{sc} \equiv \tilde{G}_0(R_j, Q_i) \tilde{S}_{Q_i} \tilde{G}_0(Q_i, T_k) \Phi_{T_k} \hat{\pi}_{T_k}$$

and the direct signals

$$\vec{Z}^{dir} \equiv \tilde{G}_0(R_j, T_k) \Phi_{T_k} \hat{\pi}_{T_k}$$

where \tilde{G}_0 is the free space vector Green's function, in an obvious shorthand notation. The objective is to identify Q_i and $\Gamma_{Q_i}(t)$ from the receiver outputs.

In the general case, the receivers R measure \vec{Z}^{sc} and \vec{Z}^{dir} , from which the required parameters are to be estimated. But suppose each R_j is able to sample only a single polarisation of the fields incident upon it,

$$Z_{proj}^{sc} \equiv \vec{Z}^{sc} \cdot \hat{\pi}_{R_j} \quad \text{and} \quad Z_{proj}^{dir} \equiv \vec{Z}^{dir} \cdot \hat{\pi}_{R_j}$$

The question arises, to what extent are class identification and parameter estimation compromised? In this paper we address the question in the context of passive radars operating in the HF and VHF bands and derive quantitative measures of the value of polarimetric information for several geometries of interest.